

Phosphorus storage dynamics and adsorption characteristics for sediment from a drinking water source reservoir and its relation with sediment compositions



Xianqiang Tang^{a,b,c,*}, Min Wu^{a,c}, Xichang Dai^a, Peihong Chai^a

^a Basin Water Environmental Research Department, Changjiang River Scientific Research Institute, Wuhan 430010, China

^b Jiangxi Provincial Research Institute of Soil and Water Conservation, Nanchang 330029, China

^c Collaborative Innovation Center for Geo-Hazards and Eco-Environment in Three Gorges Area, Hubei Province, Yichang 443002, China

ARTICLE INFO

Article history:

Received 3 August 2013

Received in revised form

20 December 2013

Accepted 1 January 2014

Keywords:

Phosphorus adsorption

Sediment composition

Fractional analysis

Amorphous iron oxides

ABSTRACT

Water and sediment samples were collected from a representative drinking water source reservoir to investigate the nutrient spatial distributions, phosphorus storage, adsorption features and its relation with sediment compositions. Monitored water TN, TP concentrations, sediment pH values exhibited a gradual decrease trend from the upstream to the downstream. Sediment AlT content (total aluminum oxides) was 2–4 times higher than FeT (total iron oxides) which mainly comprised with FeO (free iron oxides) and Feox (amorphous iron oxides). Phosphorus fractional analysis found that Ca-P was the major phosphorus component while Ex-P + Al-P + Fe-P contents accounted for no more than 20% to sediment TP. Phosphorus adsorption process followed the pseudo-second-order kinetic model and Langmuir isotherm equations better than other kinetic and isotherm models. Film-diffusion was the rate-limiting step and physic processes dominated phosphorus adsorption. Maximal phosphorus adsorption capacities could be significantly well simulated with sediment Feox, FeT and TP concentrations ($r^2 = 0.96$).

© 2014 Elsevier B.V. All rights reserved.

1. Introduction

The Danjiangkou Reservoir ($32^{\circ}36'–33^{\circ}48' \text{ N}$, $110^{\circ}59'–111^{\circ}49' \text{ E}$) has a usual water surface area of 745 km^2 and water storage capacity of 17.45 billion m^3 (Li et al., 2008). Since 2002, the Chinese government has been implementing the Middle Route Project (MRP) of the South to North Water Diversion Project (SNWDP) transferring water from the Danjiangkou Reservoir to North China, especially to Beijing and Tianjin to mitigate the crisis of water resource shortages (Fig. 1). The Danjiangkou Reservoir will have a storage capacity of approximately 33 billion m^3 when the existing dam is heightened from 145 m to 175 m (Wang and Ma, 1999). It is planned to extract 95–130 billion m^3 water a year from the Danjiangkou Reservoir since 2014, and good water quality thus determines the fates of the SNWDP.

Water eutrophication is the major risk for the Danjiangkou Reservoir (Li et al., 2009; Tang et al., 2012). As a centralized drinking water source, water quality of the Danjiangkou Reservoir

is required to match the Class II of the national standard GB 3838-2002 with total nitrogen (TN) and total phosphorus (TP) concentrations no more than 0.50 mg/L and 0.025 mg/L (Ministry of Environmental Protection, 2002), respectively. Anthropogenic inputs including agricultural runoff, urban domestic and industrial effluents contributes major nutrient loads to the Danjiangkou Reservoir. Algae blooms were already observed in 1992, 1998, 2000 and 2003 in some tributary estuaries and bays of the Danjiangkou Reservoir and phosphorus had been considered the limiting factor for algal production (Xiong and Liao, 2003). Between 2005 and 2006, water quality monitoring results further confirmed that phosphorus was the limiting nutrient factor for water eutrophication (Li et al., 2009). Increase in phosphorus concentrations implicates a great potential of algae bloom in the future considering that the water transfer project will enlarge the water storage capacity and sharply slow down the water velocity.

Release of nitrogen, phosphorus and other pollutants from submerged contaminated sediments will also potentially deteriorate water quality and threaten water supply safety. Previous studies have shown that sediment acts not only as a sink of nutrients but also as a source (Aigars and Carman, 2001). The nutrient release process has a significant impact on water quality and may result in continuous eutrophication in reservoirs, especially when external

* Corresponding author at: Basin Water Environmental Research Department, Changjiang River Scientific Research Institute, Wuhan 430010, China.
Tel.: +86 027 82926548; fax: +86 027 82605989.

E-mail address: tomxqq@gmail.com (X. Tang).

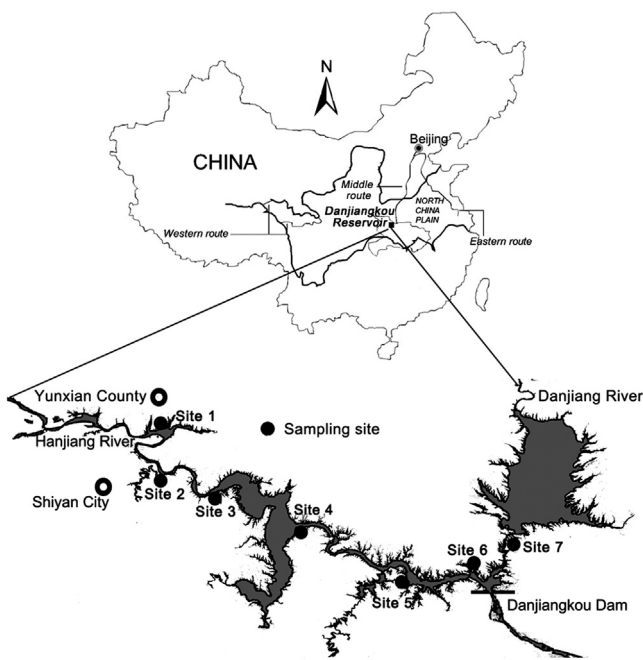


Fig. 1. Map of the Danjiangkou Reservoir showing (a) South to North Water Division Project (SNWDP) and (b) sampling sites of the water and sediment.

nutrient sources are under control. In 2010, sediment TP concentrations were firstly investigated from three representative sampling sites in the Danjiangkou Reservoir area, and recorded values ranged from 671 mg/kg to 953 mg/kg (Tang et al., 2012). High TP content in particular of loosely exchangeable phosphorus in the sediment is easily available to algae, and will therefore promote blooms after the completion of the dam heightening project.

The sorption of phosphorus on the sediments is one of the most important processes used to regulate the mobilization and dynamic behavior of phosphorus in the aquatic sediments (Appan and Wang, 2000). Mobilized sediment phosphorus may either be resorbed by other sediment components or released to the overlying water. Resorption or release mainly depends on the overall sediment compositions and phosphorus saturation (Istvánovics, 1994). It is demonstrated that phosphorus adsorption capacity is closely related to sediment composition, such as contents of organic matter, and Fe/Al oxides. In general, organic matter is positively correlated with phosphorus adsorption (Wang et al., 2009), while metals oxides play a key role in determining the phosphorus capacity because of the high specific surface of the Fe/Al hydroxides (Makris et al., 2005). Moreover, the maximal phosphorus adsorption capacity is also enhanced with the increase of the sediment total content of Fe + Al (Wang et al., 2009). For Danjiangkou Reservoir, however, the relationships between phosphorus adsorption performance and sediment compositions were not pronounced as in other freshwater bodies.

In the present study, seven representative water and surface sediment samples were collected from the Danjiangkou Reservoir to determine the nutrients in particular of phosphorus storage and spatial distribution characteristics. As a powerful method, sequential chemical extraction of phosphorus and Fe/Al oxides was conducted to explore the relationships between sediment composition variables and phosphorus storage and adsorption behavior. Finally, phosphorus adsorption process and mechanism was elucidated by batch adsorption kinetics and isotherm experiments and further mathematic model calculations.

2. Materials and methods

2.1. Water sampling and nutrient determination

In July 2012, water samples were collected from seven sampling sites 7 (Yunxian), 6 (Shendinghe), 5 (Xiaochuan), 4 (Longkou), 3 (Langhekou), 2 (Fenghuangshan) and 1 (Sigou), which were located from the upstream to the downstream of the Danjiangkou Reservoir (Fig. 1). Sampling bottles were soaked for 24 h in 10% hydrochloric acid and subsequently rinsed in pure water prior to use. According to Chinese Environmental Quality Standards for Drinking Water (GB3838-2002), 500 mL water samples were collected at an approximate depth of 30 cm with sampling sites depth of nearly 1.0 m. All water samples were analyzed on the same day for the following nutrient parameters: permanganate index (COD_{Mn}), ammonia-nitrogen ($\text{NH}_4\text{-N}$), nitrate-nitrogen ($\text{NO}_3\text{-N}$), total nitrogen (TN), soluble reactive phosphorus (SRP) and TP according to the American standard methods (APHA, 1998).

2.2. Sediment sampling and composition analysis

Once finished the water sampling work, each surface sediment samples was immediately collected at the same water sampling sites (Fig. 1) with a grab style sampler. All the surface sediment samples were transported to the laboratory within sealed plastic bags, and natural air-dried and sieved with 100 mm-diameter meshes (obtained sub-sample with grain sizes less than 0.149 mm) before analysis. pH and organic matter contents for all the samples were determined according to the Chinese Soil Physical and Chemical Standard Methods (Bao, 2000).

2.2.1. Phosphorus fractional analysis

Considering the similarities between sediment and soil, sequential extraction of phosphorus was undertaken to determine the phosphorus species according to the procedures recommended by The Chinese Soil Physical and Chemical Standard Methods (Bao, 2000). Exactly 25 mL of 1 mol/L NH_4Cl were added to 500 mg sediment (dry weight equivalent), and the suspension was shaken for 0.5 h. After shaking, the suspension was centrifuged at 3000 rpm for 10 min, and the supernatant was decanted. This process was repeated with 0.5 mol/L NH_4F (shaken for 1 h), 0.1 mol/L NaOH (shaken for 2 h, and shaken for 2 h again after standing for 16 h), 0.3 mol/L $\text{Na}_3\text{C}_6\text{H}_5\text{O}_7 \cdot 2\text{H}_2\text{O}$ (shaken for 0.5 h) and then with 0.5 mol/L H_2SO_4 (shaken for 1 h). These fractions represented exchangeable P (Ex-P), P bound by Al oxides (Al-P), P bound by Fe oxides (Fe/P), occluded phosphorus (O-P) and calcium bound P (Ca-P), respectively. The TP concentration within the sediments was determined by treating the sub-sample at 720 °C, followed by 3 mol/L H_2SO_4 extraction (Bao, 2000).

2.2.2. Fe/Al fractional analysis

Free iron oxides (Fed), amorphous iron oxides (Feox) and iron present as pyrite (FeP) were analyzed by extracting with 0.3 mol/L $\text{Na}_3\text{C}_6\text{H}_5\text{O}_7 \cdot 2\text{H}_2\text{O} + 1.0 \text{ mol/L NaHCO}_3$, 0.1 mol/L $\text{H}_2\text{C}_2\text{O}_4 \cdot 2\text{H}_2\text{O} + 0.2 \text{ mol/L } (\text{NH}_4)_2\text{C}_2\text{O}_4 \cdot \text{H}_2\text{O}$ and 0.1 mol/L $\text{Na}_4\text{P}_2\text{O}_7 \cdot 10\text{H}_2\text{O}$, iron content contained in the solution were then determined using phenanthroline spectrophotometric method (Bao, 2000). Exactly 10 mL of 1 mol/L KCl were added to 1000 mg sediment (dry weight equivalent), and the suspension was shaken for 0.5 h. After shaking, the suspension was centrifuged at 3000 rpm for 10 min, and the supernatant was decanted for aluminum contents determination using aluminon spectrophotometric method (Shao et al., 1998). This process was repeated with 0.2 mol/L HCl (shaken for 0.5 h). These fractions represent exchangeable aluminum oxides (ExAl) and adsorbed

aluminum oxides (HyAl), respectively. The total iron oxides (FeT) and total aluminum oxides (AIT) contents within the sediments was determined by treating the 500 mg sub-sample at 700 °C with the presence of 4.0 g NaOH, and then followed by 20% HCl extraction and spectrophotometric determination (Bao, 2000).

2.3. Phosphorus adsorption and process simulation

2.3.1. Description of the experiment

Batch adsorption experiments were performed to obtain kinetic and isotherm data for all sediment samples with grain sizes of less than 0.149 mm. Regardless of kinetic or isotherm adsorption, KH₂PO₄ was used as the only phosphorus source and each experiment was conducted in triplicate. For adsorption kinetic experiments, 500 mg sediment (dry weight equivalent) was placed in a 50 mL polyethylene bottles containing 25 mL of 10 mg/L phosphorus solution. Each solution was continuous shaken at 200 rpm ($r=2$) within a water batch at 25 °C for 0.0, 0.5, 1.0, 2.0, 4.0, 8.0, 12.0 and 24 h. Suspensions were centrifuged for 10 min at a speed of 3500 rpm ($r=1895$). Phosphorus remaining in the supernatant was determined according to APHA (1998).

For adsorption isotherm experiments, 500 mg sediment samples were placed in a 50 mL polyethylene bottles containing 20 mL of different initial phosphorus concentrations (0, 0.5, 1.0, 2.0, 5.0, 10.0, 25.0 and 50.0 mg/L) solution. Each solution was shaken at 200 rpm ($r=2$) within a water batch for 24 h at 25 °C. Phosphorus in suspensions was centrifuged and subsequently determined using the same procedure and method mentioned above. The adsorption capacity (mg/kg) was calculated using the following equation:

$$q_e = \frac{(C_0 - C_e)V}{W} \quad (1)$$

where C_0 and C_e were the initial and equilibrium concentrations (mg/L) of phosphorus in the solution, respectively; V was the volume of solution (L); and W is the mass of sediments used (g).

Data collected from the batch adsorption experiments were expressed as means and standard deviations (SD). Obtained data were further fitted with various adsorption kinetic and isotherm models to help understand the phosphorus adsorption process and mechanism.

2.3.2. Adsorption kinetic simulations

Pseudo-first-order and pseudo-second-order adsorption kinetic models were applied to evaluate the kinetic order of the adsorption process. The specific rate equations were shown in Eqs. (2) and (3) (Ho and McKay, 1999).

$$\log(q_e - q_t) = \log q_e - k_1 t \quad (2)$$

$$\frac{t}{q_t} = \frac{1}{k_2 q_e^2} + \frac{t}{q_e} \quad (3)$$

where q_e and q_t are adsorbed phosphorus capacity (mg/kg) at equilibrium and at time t (h), respectively; k_1 and k_2 are the rate constants of the pseudo-first-order adsorption (1 h⁻¹) and pseudo-second-order rate constant (kg/(mg h)).

The rate-limiting step of the sediment adsorption process can be calculated using the first-order kinetic data (Maji et al., 2008). Assuming spherical geometry of the adsorbent, the calculated pseudo-first-order rate constant was utilized to correlate with the pore diffusion (Eq. (4)) and film diffusion coefficients (Eq. (5)). $t_{1/2}$ is the time required to bring down the phosphorus concentration to half the initial concentration.

$$t_{1/2} = 0.03 \frac{r^2}{D_p} \quad (4)$$

$$t_{1/2} = 0.23 \frac{r\delta}{D_f} \times \frac{C_s}{C_e} \quad (5)$$

where r is the mean geometric radius of the sediment particle (cm); D_p and D_f are the pore diffusion and film diffusion coefficients (cm²/s), respectively; C_s and C_e are the concentrations of phosphorus on the adsorbent (mg/kg) and in the solution at equilibrium (mg/L); and δ was the film thickness of 0.001 cm.

The relationship between $t_{1/2}$ and k_1 (overall reaction rate constant) can be described in Eq. (6) (Asher and Pankow, 1991). Values of $t_{1/2}$ would be calculated with k_1 obtained from Eq. (2).

$$t_{1/2} = - \frac{\ln(0.5)}{k_1} \quad (6)$$

2.3.3. Adsorption isotherm simulations

Langmuir and Freundlich isotherm were used to investigate the maximum adsorption capacity of different sediments samples. The linear forms of Langmuir and Freundlich equations were expressed in Eqs. (7) and (8).

$$\frac{C_e}{q_e} = \frac{C_e}{q_m} + \frac{1}{k_L q_m} \quad (7)$$

$$\ln q_e = \ln k_F + \frac{1}{n} \ln C_e \quad (8)$$

where C_e is the equilibrium phosphorus concentration (mg/L), q_e is the adsorption capacity at equilibrium (mg/kg), q_m is the theoretical maximal capacity (mg/kg), k_L is the Langmuir sorption equilibrium constant (L/mg) related to the adsorption energy, k_F is the equilibrium constant indicative of adsorption capacity, and n is the adsorption equilibrium constant whose reciprocal is indicative of adsorption intensity (Li et al., 2012).

In order to understand the type of phosphorus adsorption to different sediments samples, the data were applied to Dubinin–Radushkevich (D–R) isotherm (Kundu and Gupta, 2006), which can be expressed as Eqs. (9) and (10).

$$\ln q_e = \ln q_m - k_{DR} \varepsilon^2 \quad (9)$$

$$\varepsilon = RT \ln \left(1 + \frac{1}{C_e} \right) \quad (10)$$

where q_e was the adsorption capacity at equilibrium (mg/kg), q_m is the maximal capacity (mg/kg), C_e is the equilibrium phosphorus concentration (mg/L), k_{DR} is the constant related to adsorption energy (mol²/kJ²), R is the universal gas constant of 8.3145 kJ/(mol K) and T is the experimental temperature of 298 K in this study.

k_{DR} shows the mean free energy of the adsorption per molecule when it is transferred to the surface of the solid from the solution, and can be calculated using Eq. (11), where E is the mean sorption energy (kJ/mol) providing important information about physical and chemical nature of the adsorption process.

$$E = \frac{1}{\sqrt{2k_{DR}}} \quad (11)$$

2.4. Statistical analysis and simulation

Data collected from the sediment composition analysis and phosphorus adsorption calculation were used for statistical analysis and mathematic simulation. All statistical tests were performed with the software SPSS (SPSS, 2003) including multivariable correlation matrix calculation and stepwise linear regression analysis. Correlation coefficients (r^2) and p value were obtained to assess

the linear relationships between variables. Relationships among the considered variables were tested with significance set at $p < 0.05$.

3. Results and discussion

3.1. Nutrient dynamics in water

Nutrient variables showed obviously spatial variability for different sampling sites. Except for Shendinghe, concentrations of nitrogen or phosphorus variables decreased in general from the upstream to the downstream (Table 1). Decline in water flow velocity and dilution of the main water column probably stimulated the nutrient sedimentation, diffusion and transportation, and thus caused continuously nutrient attenuation. In general, $\text{NO}_3\text{-N}$ was higher than $\text{NH}_4\text{-N}$ except for the sampling site Shendinghe. Upstream nitrogen fertilizer loss, and atmospheric nitrogen fixation by phytoplankton greatly increase the nitrogen input to the reservoir (Tang et al., 2012), and all the inorganic nitrogen parameters were higher than SRP, which is the major component of TP (Table 1).

As a centralized drinking water source, water quality of the Danjiangkou Reservoir was required to match the Class II of the national standard GB 3838-2002 (Ministry of Environmental Protection, 2002). Except for sampling site Shendinghe, COD_{Mn} and $\text{NH}_4\text{-N}$ were generally good, up to class II of the national standard. TN concentrations for all of the sampling sites greatly exceeded the limitations of 0.50 mg/L. Only three sampling sites including Langhekou, Fenghuangshan and Sigou had TP levels of less than 0.025 mg/L, which was up to class II of the national standard.

Higher nutrient concentrations usually occurred in areas of intensive urban and agricultural activities (Wu et al., 2013). Sampling sites Yunxian and Shendinghe were major outlet of urban domestic wastewater and agricultural runoff for upstream Yunxian County and Shiyan City. Xiaochuan was located in the traditional fish farming area with developed cage aquaculture industry. Therefore, these areas contributed large amount of nitrogen and phosphorus into the water (Li et al., 2009; Tang et al., 2012). Phosphorus had been already identified as the limiting factor for algal production in the estuary of Danjiangkou Reservoir (Li et al., 2009; Xiong and Liao, 2003). Once the water column phosphorus loads exceeded the critical value of 0.02 mg/L for algae bloom, TN:TP ratio would play a key role in regulating the algae propagation. In this study, the average TN:TP ranged from 7.9 to 20.1 for sampling sites Yunxian, Shendinghe and Xiaochuan, which corresponded well with the critical TN:TP ratios for algal bloom from 10:1 to 32:1 in the environment (Pu et al., 2000). Thus, there is great risk of algal bloom in the future considering that the dam heightening project will enlarge the water storage capacity and sharply slow down the water velocity.

Table 1

Mean concentrations \pm SD for COD_{Mn} , $\text{NH}_4\text{-N}$, $\text{NO}_3\text{-N}$, TN, SRP and TP in the Danjiangkou Reservoir water.

Sampling site	Variables					
	COD_{Mn} (mg/l)	$\text{NH}_4\text{-N}$ (mg/l)	$\text{NO}_3\text{-N}$ (mg/l)	TN (mg/l)	SRP (mg/l)	TP (mg/l)
Yunxian	4.58 \pm 0.12	0.24 \pm 0.04	1.18 \pm 0.10	1.61 \pm 0.10	0.16 \pm 0.01	0.20 \pm 0.02
Shendinghe	7.44 \pm 0.14	4.91 \pm 0.10	1.72 \pm 0.12	7.84 \pm 0.21	0.30 \pm 0.02	0.39 \pm 0.04
Xiaochuan	2.72 \pm 0.11	0.17 \pm 0.03	1.22 \pm 0.08	1.47 \pm 0.08	0.07 \pm 0.01	0.08 \pm 0.01
Longkou	3.36 \pm 0.12	0.13 \pm 0.04	0.91 \pm 0.09	1.40 \pm 0.07	0.02 \pm 0.01	0.03 \pm 0.01
Langhekou	2.80 \pm 0.10	0.15 \pm 0.03	0.78 \pm 0.10	1.32 \pm 0.11	0.017 \pm 0.01	0.02 \pm 0.01
Fenghuangshan	2.64 \pm 0.12	0.16 \pm 0.04	0.82 \pm 0.07	1.18 \pm 0.09	<0.01	<0.01
Sigou	2.36 \pm 0.14	0.10 \pm 0.04	1.05 \pm 0.12	1.46 \pm 0.13	<0.01	<0.01

COD_{Mn} : chemical oxygen demand (permanganate); $\text{NH}_4\text{-N}$: ammonia-nitrogen; $\text{NO}_3\text{-N}$: nitrate-nitrogen; TN: total nitrogen; SRP: soluble reactive phosphorus; TP: total phosphorus.

3.2. Sediment composition characteristics

Sediment pH values, OM and Fe/Al oxides fractional contents were given in Table 2. Sediments pH values ranged from 5.56 to 6.24, and showed a general decrease tend from the upstream to the downstream. Plenty of rainfall and rich of Fe and Al oxides may cause the weak acid sediment environments as reported elsewhere (Wang et al., 2011). Organic matter, exhibited a rising concentrations range from 2.13% to 6.94% with the decrease in sampling distance from the dam (Table 2). The pattern of OM distribution can be explained by the slow flow velocity resulting in nutrient accumulation with the presence of dam (Wu et al., 2011).

Metal oxides (Fe and Al) had been considered to be a main factor that determines phosphorus retention because of the high specific surface of the hydroxides (Wang et al., 2009). As shown in Table 2, FeP accounted for negligible part of the FeT storage while Fed and Feox were the major iron oxide compositions in tested sediment samples. Fed was invariably the dominated form of iron oxide, with most value exceeding 40.65% observed in Longkou, relative high Fed contents might determine the sediment phosphorus geochemical circulation in the Danjiangkou Reservoir.

Huge surface area of Feox facilitated the phosphorus adsorption when compared to Fed (Baldwind, 1996), and was considered the main factor to determine the phosphorus mobility. In the present study, Feox/FeT ranged from 3.85% to 18.01% (Table 2), and its variability was probably originated from the difference in sediment organic matter, water trophic state and chemistry. Feox was the main variable to retain phosphorus dissolved in water body or mineralized from organic matter (Zhou et al., 2005). Sediment with high Feox/FeT ratio had much better ability to trap dissociative phosphorus and establish the large pool of available phosphorus.

Aluminum oxides also greatly impacted on sediment phosphorus storage, distribution and adsorption. In the present study, sediment AIT contents showed significantly higher levels than FeT concentrations, and the maximal value of 252.74 g/kg was recorded for Longkou sampling site (Table 2). Although ExAl contributed less than 0.01% of AIT (Table 2), it was closely related to the aluminum circle and transfer within soil and nature water bodies, and was of great importance to regulate the soil acid (Shao et al., 1998). Sediment ExAl concentrations decreased with decline in corresponding pH values (Table 2), and little ExAl could be detected if soil pH less than 5.5 (Soon, 1993). HCl extracted HyAl mainly consisted of hydroxyl-aluminum, aluminum hydroxide and parts of amorphous aluminosilicate adsorbed on the sediment surface in the form of inorganic film (Shao et al., 1998). As parts of active aluminum oxides, sediment HyAl content was regarded as a parameter to evaluate the sediment phosphorus adsorption performance (Shao et al., 1998). No obvious relationship between HyAl and AIT contents was observed in the present study, which compared well elsewhere with the fact that HyAl contents mostly determined by soil parent material (Wang, 1995).

Table 2

Mean values \pm SD for pH, OM, FIO, AIO, TIO, AAO, TAO in the Danjiangkou Reservoir surface sediment.

Sampling site	Variables								
	pH (-)	OM (%)	FeP (mg/kg)	Fed (g/kg)	Feox (g/kg)	FeT (g/kg)	ExAl (mg/kg)	HyAl (g/kg)	AIT (g/kg)
Yunxian	6.24 \pm 0.13	2.13 \pm 0.24	12.07 \pm 1.38	11.70 \pm 0.65	8.08 \pm 0.26	45.86 \pm 2.13	11.74 \pm 0.84	2.65 \pm 0.25	163.50 \pm 12.35
Shendinghe	6.05 \pm 0.11	2.85 \pm 0.17	27.40 \pm 4.19	14.77 \pm 0.52	7.38 \pm 0.37	58.31 \pm 2.74	15.84 \pm 1.87	5.16 \pm 0.61	188.56 \pm 13.64
Xiaochuan	6.04 \pm 0.12	3.74 \pm 0.23	41.00 \pm 6.63	15.00 \pm 0.74	9.80 \pm 0.45	54.41 \pm 1.92	12.22 \pm 1.16	3.17 \pm 0.27	148.71 \pm 11.38
Longkou	5.48 \pm 0.10	4.39 \pm 0.18	8.23 \pm 0.87	26.09 \pm 0.99	5.42 \pm 0.56	64.17 \pm 3.11	9.81 \pm 0.79	3.39 \pm 0.33	252.74 \pm 18.19
Langhekou	5.81 \pm 0.12	5.28 \pm 0.31	29.29 \pm 3.26	14.95 \pm 0.80	8.28 \pm 0.52	53.19 \pm 1.90	9.32 \pm 0.68	2.58 \pm 0.19	211.20 \pm 17.73
Fenghuangshan	5.56 \pm 0.12	6.21 \pm 0.42	8.23 \pm 0.91	15.67 \pm 0.97	3.58 \pm 0.41	93.46 \pm 4.52	7.87 \pm 0.82	2.30 \pm 0.34	199.13 \pm 13.27
Sigou	5.65 \pm 0.14	6.94 \pm 0.54	48.48 \pm 5.37	15.91 \pm 1.12	7.85 \pm 0.68	53.19 \pm 2.93	9.08 \pm 1.10	3.54 \pm 0.52	207.46 \pm 15.61

OM: organic matter; FeP: iron present as pyrite; Fed: free iron oxides; Feox: amorphous iron oxides; FeT: total iron oxides in the sediment; ExAl: exchangeable aluminum oxides; HyAl: adsorbed aluminum oxides; AIT: total aluminum oxides.

3.3. Sediment phosphorus storage

In the present study, Ex-P contents ranged from 0.74 mg/kg to 3.57 mg/kg and exhibited a decline trend from the upstream to the downstream (Table 3). Fe-P distribution was irregular, and the maximal and minimal Fe-P concentrations of 67.03 mg/kg and 5.73 mg/kg were recorded at Longkou and Yunxian sampling sites, respectively. Fe-P concentration was significantly and positively related to sediment Fed contents at $p < 0.05$ (Table 4). Compared to Fe-P, distribution of Al-P was quite uniform and fell in the range of 10.50–19.08 mg/kg, correlation analysis results indicated that Al-P were weakly and positively related to ExAl, HyAl and AIT variables at $p > 0.05$ (Table 4). Ca-P and O-P were invariably higher than other phosphorus fractions. Ca-P was the major component of TP, and had correlation coefficient of 0.984 to TP at $p < 0.05$ (Table 4). However, O-P was insignificantly related to any sediments compositions.

Ratio of each phosphorus fraction to TP within the sediment samples were shown in Fig. 2. The Ex-P content contributed to less than 0.5% of TP, the Fe-P and Al-P proportions related to TP were roughly ranged from 0.82% to 14.33%, and from 1.64% to 4.08%, respectively. The Ca-P fraction was invariably the dominant form of phosphorus, with most values exceeding 70%. O-P was the second contributor to TP, and accounted for 11.64–31.61% in TP concentrations.

Soluble exchangeable phosphorus was the most immediately available phosphorus within sediments (Ribeiro et al., 2008). Ex-P was the best parameter for the assessment of the bioavailability of phosphorus. Ex-P level measured within Danjiangkou Reservoir sediments was no more than 3.57 mg/kg (Table 3), and great lower compared with reported values range from 13 mg/kg to 59 mg/kg (Ribeiro et al., 2008). Relatively high Ex-P concentrations observed in Yunxian, Shendinghe and Xiaochuan means that loosely exchangeable phosphorus will be easily available to algae, consequently promoting blooms in these areas.

Fe-P and Al-P represented phosphorus bond to iron and aluminum oxides and was exchangeable with OH- and other inorganic phosphorus compounds, which were soluble in bases (Kozerski and

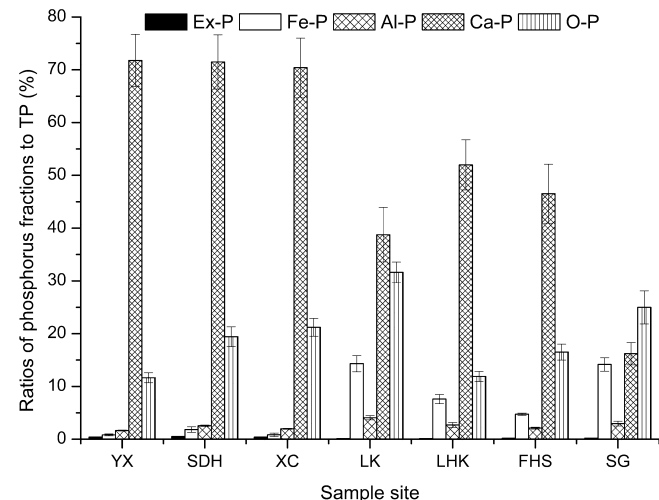


Fig. 2. Ratios of individual phosphorus fractions to total phosphorus (TP) in the sediment collected from the Danjiangkou Reservoir. YX, SDH, XC, LK, LHK, FHS and SG are short for Yunxian, Shendinghe, Xiaochuan, Longkou, Langhekou, Fenghuangshan and Sigou, respectively.

Kleberg, 1998). Previous research indicated that Fe-P and Al-P supported growth of phytoplankton, and could also be used for the evaluation of algal available phosphorus (Zhou et al., 2001). Fe-P and Al-P concentrations were generally higher in eutrophic and non-calcareous environments with the highest proportions of 70% (Penn et al., 1995). In the Danjiangkou Reservoir, mesotrophy state may result in no more than 20% of Fe-P + Al-P to TP (Fig. 2).

Ca-P was generally considered as a major storage fraction of sedimentary phosphorus with low mobile potentials (Gomez et al., 1999). Similar to the result of this study, high proportions of calcium mineral-P were observed within rivers and lakes with various trophic statuses (Jin et al., 2006; Tian and Zhou, 2007). For these studies, Ca-P fractions were dominant, contributing 35–70% of TP, with calcareous sediments close to the upper limit of this range (Jin

Table 3

Mean concentrations \pm SD for Ex-P, Fe-P, Al-P, Ca-P, O-P, TP in the Danjiangkou Reservoir surface sediment.

Sampling site	Variables					
	Ex-P (mg/kg)	Fe-P (mg/kg)	Al-P (mg/kg)	Ca-P (mg/kg)	O-P (mg/kg)	TP (mg/kg)
Yunxian	2.94 \pm 0.33	5.73 \pm 1.37	11.45 \pm 0.63	500.27 \pm 48.46	81.11 \pm 6.53	697.00 \pm 61.28
Shendinghe	3.57 \pm 0.41	12.64 \pm 3.57	17.65 \pm 0.92	491.43 \pm 35.33	133.59 \pm 12.84	687.46 \pm 56.79
Xiaochuan	3.25 \pm 0.62	6.92 \pm 2.82	16.22 \pm 0.84	578.38 \pm 62.43	174.15 \pm 13.86	821.43 \pm 79.32
Longkou	0.63 \pm 0.18	67.03 \pm 7.16	19.08 \pm 1.79	181.30 \pm 24.16	147.91 \pm 9.13	467.85 \pm 47.23
Langhekou	0.84 \pm 0.32	45.80 \pm 5.31	16.22 \pm 2.83	312.70 \pm 28.57	71.57 \pm 5.76	601.52 \pm 42.15
Fenghuangshan	1.05 \pm 0.29	26.72 \pm 1.26	11.93 \pm 1.07	262.10 \pm 31.45	93.04 \pm 8.52	563.33 \pm 50.03
Sigou	0.74 \pm 0.14	50.10 \pm 4.53	10.50 \pm 1.62	57.25 \pm 7.48	88.27 \pm 11.13	353.28 \pm 27.48

Ex-P: exchangeable phosphorus; Fe-P: iron oxides bound phosphorus; Al-P: aluminum oxides bound phosphorus; Ca-P: calcium bound phosphorus; O-P: occluded phosphorus; TP: total phosphorus.

Table 4
Person correlation matrix for surface sediments collected from the Danjiangkou Reservoir.

Variable	q_m	pH	OM	FeP	Fed	Feox	FeT	ExAl	HyAl	AIT	Ex-P	Fe-P	Al-P	Ca-P	O-P	TP	E
q_m	1.000	-0.672	0.676	0.414	0.567	0.844**	-0.112	-0.495	0.448	0.622	-0.715	0.829*	-0.037	-0.831*	-0.013	-0.813*	-0.614
pH	1.000	-0.791*	0.169	-0.728	0.752	-0.616	0.713	-0.179	-0.824*	0.875**	-0.843*	-0.073	0.850*	0.041	0.772*	0.198	
OM	1.000	0.285	0.215	0.843**	0.459	-0.777*	0.313	0.459	-0.807	0.616	-0.355	-0.819*	-0.331	-0.727	-0.373		
FeP	1.000	-0.304	0.485	-0.484	0.161	0.362	-0.311	0.124	-0.053	-0.140	-0.037	0.114	-0.031	-0.841*			
Fed	1.000	0.478	0.251	-0.262	0.122	0.811*	0.531	0.771*	0.573	-0.509	0.429	-0.482	-0.207				
Feox	1.000	-0.869*	0.456	0.389	0.575	0.500	-0.366	0.066	0.485	0.174	0.460	-0.480					
FeT				-0.439	-0.404	0.281	-0.351	0.133	-0.075	-0.281	0.001	-0.196	0.295				
ExAl				1.000	-0.309	-0.444	0.877**	-0.592	0.419	0.708	0.460	0.602	-0.103				
HyAl				1.000	0.337	-0.473	0.526	0.247	-0.274	-0.278	-0.209	-0.477					
AIT					1.000	-0.794*	0.934**	0.329	-0.786*	-0.126	-0.776*	-0.106					
Ex-P						1.000	-0.890**	0.137	0.905**	0.417	0.833*	0.101					
Fe-P							1.000	0.213	-0.867*	-0.140	-0.833*	-0.312					
Al-P								1.000	0.248	0.641	0.266	-0.307					
Ca-P									1.000	0.375	0.984**	0.211					
O-P										1.000	0.395	-0.396					
TP											1.000	0.175					
E												1.000					

q_m : maximal phosphorus adsorption capacity (mg/kg); OM: organic matter (%); Fed: iron present as pyrite (mg/kg); Feox: amorphous iron oxides (g/kg); FeT: total iron oxides (g/kg); ExAl: exchangeable aluminum oxides (mg/kg); HyAl: total aluminum oxides (g/kg); AIT: total aluminum bound phosphorus (mg/kg); O-P: calcium bound phosphorus (mg/kg); Ca-P: calcium bound phosphorus (mg/kg); TP: total phosphorus (mg/kg); E: adsorption free energy (kJ/mol).

* Correlation are significant at $P=0.05$.

** Correlation are significant at $P=0.01$.

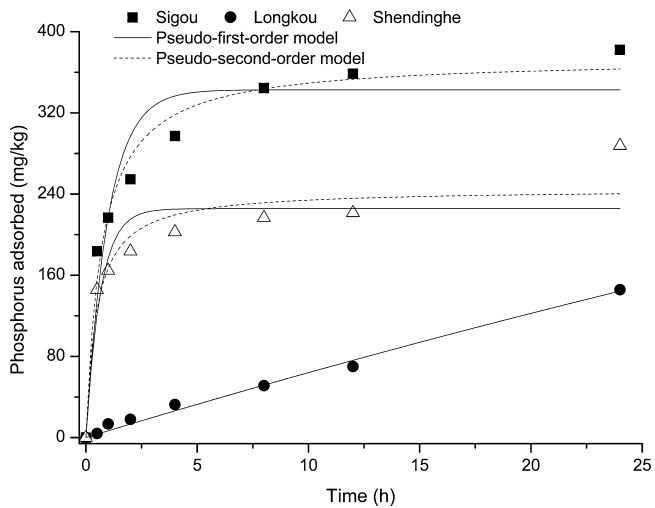


Fig. 3. Adsorption kinetics of phosphorus on the different sediments collected from the Danjiangkou Reservoir.

et al., 2006; Tian and Zhou, 2007). Though buried Ca-P was stable, but had the ability of releasing phosphorus in acid environments due to the acid decomposition effect, and exhibiting the highest release capacity of 92% at pH 5 (Peng et al., 2007).

O-P represented the inertia phosphorus fraction bound to hydrous iron oxides, and was very stable and not easy to be utilized by algae and phytoplankton (Ji et al., 2009). O-P contents usually ranged from 44 mg/kg to 243 mg/kg for natural lake sediments (Peng et al., 2009). And our measured content (71.57–174.15 mg/kg, Table 3) was in that range. Level of O-P stored within sediment directly reflects the amount of natural phosphorus input to the receiving water body (Zhang et al., 2012). In the present study, it can be concluded that phosphorus was mainly of detrital origin (Ca-P + O-P), whereas Ex-P + Fe-P + Al-P (less than 20%) originated less from detritus but more from anthropogenic sources (Ruban et al., 2001).

3.4. Phosphorus adsorption behavior and mechanism

Three sampling sites were chosen to test the difference in phosphorus adsorption kinetics among upstream, midstream and downstream sediments. Uptake of phosphorus by sediment was time dependant and increased with reaction time, and the adsorption of phosphorus was rapid in the first one hour and then slowed down when equilibrium was reached (Fig. 3). There was great variability in the adsorption process; phosphorus adsorption on sediments collected at Sigou and Shendinghe approached the equilibrium much faster than Longkou.

Further kinetic simulation results indicated that the pseudo-second-order equation was suitable for describing phosphorus adsorption (Table 5). Assuming that all the sediment particles had the same mean geometric radius of 0.149 mm, and calculated coefficients for determining the phosphorus adsorption rate limiting steps were shown in Table 6. The pore diffusion constants and film diffusion constants ranged from 0.027×10^{-8} cm²/s to 0.41×10^{-8} cm²/s, and from 0.028×10^{-8} cm²/s to 1.51×10^{-8} cm²/s, respectively. For film diffusion to be the adsorption rate-limiting step, the value of the film diffusion co-efficient (D_f) should be in the range of 10^{-8} to 10^{-6} cm²/s, and for pore diffusion to be rate-limiting, the pore diffusion coefficient (D_p) should be in the range of 10^{-13} to 10^{-11} cm²/s (Babatunde and Zhao, 2010). In the present study, film diffusion appeared to be the rate-limiting step for the phosphorus

Table 5

Comparison of the pseudo-first- and second-order reaction rate constants for different surface sediment collected from the Danjiangkou Reservoir.

Sediment	Pseudo-first-order			Pseudo-second-order		
	k_1	q_e	r^2	k_2	q_e	r^2
Shendinghe	1.54	225.62	0.85	0.0087	244.92	0.92
Longkou	0.01	739.56	0.99	3.57E-6	1370.633	0.99
Sigou	1.01	342.65	0.92	0.0038	373.75	0.98

Table 6

Calculated pore diffusion and film diffusion constants for representative surface sediments collected from the Danjiangkou Reservoir.

Parameters	Sampling site		
	Shendinghe	Longkou	Sigou
C_e (mg/L)	5.49	7.11	3.15
k_1 ($\times 10^{-3}$ s $^{-1}$)	0.43	0.0028	0.28
$t_{1/2}$ ($\times 10^3$ s $^{-1}$)	1.62	249.53	2.47
r (cm)	0.0149	0.0149	0.0149
D_p ($\times 10^{-8}$ cm 2 /s)	0.41	0.027	0.27
D_f ($\times 10^{-8}$ cm 2 /s)	0.87	0.028	1.51

adsorption kinetic process (Table 6). Considering the difference in sediment samples, further particle size analysis was recommended to obtain the actual mean geometric radius, and correct above calculated kinetic adsorption coefficients.

Different sediment compositions caused the variability in phosphorus adsorption capacities (Fig. 4 and Table 7); e.g., the maximum phosphorus adsorption capacities (obtained by the Langmuir equation) were 575.88 mg/kg for Sigou sediment in comparison with 72.96 mg/kg for Yunxian sediment. Phosphorus adsorption capacities of all tested sediment samples can be best explained by the Langmuir adsorption isotherm when compared to other two adsorption models with the corresponding correlation coefficients (r^2) were fell in the range from 0.76 to 0.98 (Table 7).

The magnitude of the mean free energy (E) of phosphorus adsorption was calculated using the Dubinin–Radushkevich (D–R) isotherm (Table 7). The value of E varied from 0.47 kJ/mol to 3.54 kJ/mol for tested sediment samples. The mean adsorption energy findings provided important information about the physical and chemical nature of the adsorption process. If $E < 8$ kJ/mol, physical adsorption dominated the adsorption process (Argun et al., 2007). Based on the judgment rule, physical processes determined

the phosphorus adsorption onto the sediments collected from the Danjiangkou Reservoir. Moreover, it can be shown that sediments with smaller mean adsorption energy may have higher maximum adsorption capacities (Table 7).

3.5. Relation of phosphorus adsorption to sediment composition

A linear regression analysis was initiated to test the relationships between q_m (obtained by Langmuir equation) and each sediment composition variables. The coefficients of the corresponding correlation matrix for all the variables were shown in Table 4. q_m was positively correlated to Feox, Fe-P, OM, AIT, Fed, HyAl and FeP; and negatively correlated to Ca-P, TP, Ex-P, pH, E and ExAl. Very weak correlations between q_m and Al-P, O-P and FeT were found (Table 4). Using a stepwise liner regression method, q_m was significantly correlated with the major sediment composition variables as following:

$$q_m = 53.81 * \text{Feox} - 0.62 * \text{TP} - 3.93 * \text{FeT} + 487.71 \quad (r^2 = 0.96)$$

Many previous studies had been conducted to assess the impact of pH and sediment compositions including OM, iron and aluminum oxides on phosphorus adsorption performance (Zhou et al., 2005; Naoml and Patrick, 1991; Wang et al., 2007). The effects of pH on lacustrine phosphorus cycling depend partly on the direct, short term effects on sorption equilibria and kinetics, as well as on the long-term effects on organic mineralization and sediment composition (Naoml and Patrick, 1991). Moreover, increase in negative charge reduced the sorption of phosphate on sediment surface when pH increased (Zhou et al., 2005), which could partly explain the negative relationships between q_m and sediment pH value (Table 4).

Sediment composition was more important than pH in impacting on phosphorus adsorption on natural sediments. Phosphorus adsorption capacity correlated well with sediment compositional characteristics such as organic matter and iron, aluminum contents (Naoml and Patrick, 1991). Positive correlation of organic matter with phosphorus adsorption was widely known (Wang et al., 2007). Active Fe and Al (i.e., in amorphous forms) played a major role in phosphorus adsorption on natural sediments, and reported positive correlation coefficients between q_m and active Fe + Al can reach 0.89 for Taihu Lake sediments (Zhou et al., 2005). Similar finding was also obtained for the Three George Reservoir sediments, where q_m greatly enhanced with increase in the total content of FeT + AIT (Wang et al., 2009). In the present study, q_m was positively related to organic matter, iron and aluminum oxides in particular of active iron oxides (Feox) (Table 4).

During the phosphorus adsorption process, iron and aluminum were prone to form different compounds besides physical adsorption. Amorphous hydrous ferric oxide (FeOOH) and hydrous aluminum oxide (AlOOH) were promising effective sites for phosphorus adsorption (Zhou et al., 2005). The iron (III) oxide surface had a high affinity for phosphorus and was capable of forming inner-sphere bidentate binuclear P–Fe (III) (Borggaard et al., 2004). Phosphorus adsorption by iron complexes occurred by ligand exchange of phosphorus for (OH)₂ and OH⁻ in the coordination spheres of surface structural Fe atoms (Babatunde and Zhao, 2010).

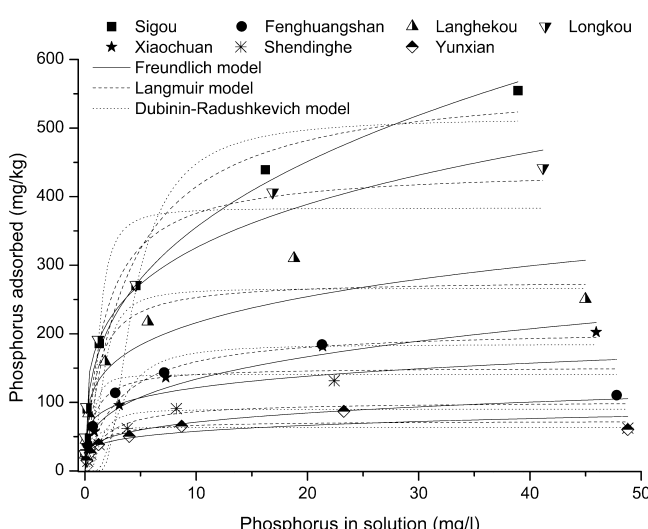


Fig. 4. Adsorption isotherm of phosphorus on the different sediments collected from the Danjiangkou Reservoir.

Table 7

Parameters of the Langmuir, Freundlich and Dubinin–Radushkevich (D–R) isotherm for different surface sediment samples collected from the Danjiangkou Reservoir.

Sampling site	Langmuir isotherm			Freundlich isotherm			Dubinin–Radushkevich (D–R) isotherm			
	q_m (mg/kg)	k_L (L/mg)	r^2	n	k_F (mg/kg)	r^2	q_m (mg/kg)	k_{DR} (mol ² /kj ²)	r^2	E (kJ/mol)
Yunxian	72.96	1.00	0.90	4.98	36.41	0.81	63.52	0.04	0.59	3.54
Shendinghe	101.51	0.57	0.76	4.03	40.16	0.55	90.09	0.24	0.56	1.44
Xiaochuan	207.63	0.33	0.98	3.17	64.77	0.97	184.59	1.15	0.81	0.66
Longkou	442.11	0.56	0.95	3.90	180.38	0.98	383.35	0.17	0.83	1.71
Langhekou	278.43	0.99	0.95	4.27	125.96	0.88	266.30	0.29	0.78	1.31
Fenghuangshan	151.18	1.32	0.87	5.37	79.05	0.72	140.71	0.06	0.69	2.89
Sigou	575.88	0.26	0.96	2.90	160.77	0.99	514.87	2.27	0.76	0.47

After relating phosphorus maximum adsorption capacity to the active iron contents (Feox), it is apparently shown that sediments with higher Feox concentrations cause higher maximum adsorption capacities (**Tables 2** and **7**).

Phosphorus fractions affected adsorption process may be the indirect response to sediment E_h variations. In adsorption experiments with anaerobic sediment being transferred to aerobic conditions, Fe (II) was oxidized to Fe (III) at the same time (**Yamada et al., 1987**). Fe (III) can adsorb a large quantity of phosphorus by forming Fe (OOH)-P complexes or precipitates (**Zak and Gelbrecht, 2002**). Therefore, conversion of Fe-P fraction (mainly existing as Fe (II)-P) into Fe (III)-P would lead to the improvement in phosphorus adsorption. Compared to active Fe-P, stable Ca-P was mainly formed through precipitation between calcite and phosphorus (**Berga et al., 2004**). High Ca-P contents in sediment usually implied long history of phosphorus pollution and poor phosphorus adsorption capacity (**Wu et al., 2011**), and decline in phosphorus adsorption sites accompanied with Ca-P formation process may be the possible reason for negatively relationships between q_m and Ca-P as observed in the present study (**Ulén and Snäll, 2007**). Relative high ratio of TN:TP implied that algal bloom has great potential to outburst in the future considering that the dam heightening project will enlarge the water storage capacity and dramatically slow down the water velocity.

3.6. Importance of phosphorus storage dynamics and adsorption characteristics

Phosphorus flux control was of great importance to prevent algae bloom in the Danjiangkou Reservoir. Excessive nutrient input from the upstream basin resulted in 0.2 mg/L higher water column phosphorus for sampling sites Yunxian and Shendinghe (**Table 1**). It was necessary to reduce the phosphorus discharge from the upstream urban and agricultural areas. Release of active sediment Ex-P, Fe-P and Al-P would partly increase the water column phosphorus bioavailability. Acid sediment environment also favored the decomposition of abundant Ca-P (**Peng et al., 2007**). It is implied that sediment Ca-P should be considered as a potential phosphorus release “source” in the Danjiangkou Reservoir. Sediment exhibited excellent phosphorus adsorption performance, and should be a “sink” for water column phosphorus in the short term. However, sediment phosphorus adsorption characterized as unstable physical adsorption, which was difficult in reducing the sediment phosphorus mobility. Therefore, reduction of phosphorus source input, increase in sediment alkalinity was crucial to protect the Danjiangkou Reservoir water quality.

4. Conclusions

Spatial pattern of nutrient distribution was evident, and higher nutrient concentrations occurred in the upstream urban and agricultural production areas. Sediment pH values and OM contents were continuously decreased and increased from the upstream to

downstream, respectively. Feo was invariably the dominant iron oxides compared to Feox and FeP. Sediment Ca-P contributed most to TP loads, and inorganic active Ex-P, Fe-P and Al-P accounted for no more than 20% of sediment TP. Phosphorus adsorption kinetics and isotherm can well fitted by pseudo-second-order equation and Langmuir equation, respectively. Film diffusion was the major phosphorus adsorption rate limiting steps and physic adsorption dominated the sorption of phosphorus onto the sediments. Maximal phosphorus adsorption capacity can well simulated with sediment Feox, FeT and TP concentrations.

Acknowledgements

This study was supported by National Natural Science Foundation of China (No. 51209011 and 51379017), Jiangxi Provincial Research Institute of Soil and Water Conservation Open Research Project (No. JXSB201206), “948” Imported Project of Ministry of Water Resource (No. 201208), and Special Funds for Technology Research and Development of Ministry of Science and Technology (No. 2012EG136134). We also express great appreciations to the reviewers and editors whose comments were important in clarifying this paper.

References

- Aigars, J., Carman, R., 2001. Seasonal and spatial variations of carbon and nitrogen distribution in the surface sediments of the Gulf of Riga, Baltic Sea. *Chemosphere* 43, 313–320.
- APHA., 1998. Standard Methods for the Examination of Water and Wastewater, 20th ed. American Public Health Association/American Water Works Association/Water Environment Federation, Washington DC, USA.
- Appan, A., Wang, H., 2000. Sorption isotherms and kinetics of sediment phosphorus in a tropical reservoir. *J. Environ. Eng.* 126, 993–998.
- Argun, M.E., Dursun, S., Ozdemir, C., Karatas, M., 2007. Heavy metal adsorption by modified oak sawdust: thermodynamics and kinetics. *J. Hazard. Mater.* 141, 77–85.
- Asher, W.E., Pankow, J.F., 1991. Prediction of gas/water mass transport coefficients by a surface renewal model. *Environ. Sci. Technol.* 25, 1294–1300.
- Babatunde, A.O., Zhao, Y.Q., 2010. Equilibrium and kinetic analysis of phosphorus adsorption from aqueous solution using waster alum sludge. *J. Hazard. Mater.* 184, 746–752.
- Baldwind, S., 1996. The phosphorus composition of a diverse series of sediments. *Hydrobiologia* 335, 63–73.
- Bao, S.D., 2000. Soil and Agricultural Chemistry Analysis. Chinese Agriculture Publishing House, Beijing, China (in Chinese).
- Berga, U., Thomas, N., Dietfried, D., Rolf, N., Doris, S., 2004. Sediment capping in eutrophic lakes: efficiency of undisturbed calcite barriers to immobilize phosphorus. *Appl. Geochem.* 19, 1759–1771.
- Borggaard, O.K., Raben-Lange, B., Gimsing, A.L., Strobel, B.W., 2004. Influence of humic substances on phosphate adsorption by aluminium and iron oxides. *Geoderma* 127, 270–279.
- Gomez, E., Durillon, C., Rofes, G., Picot, B., 1999. Phosphate adsorption and release from sediments of brackish lagoons: pH, O₂, and loading influence. *Water Res.* 33, 2437–2447.
- Ho, Y.S., McKay, G., 1999. Pseudo-second order model for sorption processes. *Process. Biochem.* 34, 451–465.
- Istvánovics, V., 1994. Fractional composition, adsorption and release of sediment phosphorus in the Kis-Balaton Reservoir. *Water. Res.* 28, 717–726.
- Ji, F.Y., Cao, L., Lin, M., Wang, T.J., Li, S., 2009. Phosphorus forms analysis in sediments of the newly emerged fluctuation zone in Three Gorges Reservoir area. *Res. Environ. Sci.* 8, 882–886 (in Chinese).

- Jin, X.C., Wang, S.R., Pang, Y., Wu, F.C., 2006. Phosphorus fractions and the effect of pH on the phosphorus release of the sediments from different trophic areas in Taihu Lake, China. *Environ. Pollut.* 139, 288–295.
- Kozerski, H.P., Kleeberg, A., 1998. The sediments and the benthic pelagic exchange in the shallow lake Muggelsee. *Int. Rev. Hydrobiol.* 83, 77–112.
- Kundu, S., Gupta, A.K., 2006. Adsorptive removal of As (III) from aqueous solution using iron oxide coated cement (IOCC): evaluation of kinetic, equilibrium and thermodynamic models. *Sep. Purif. Technol.* 51, 165–172.
- Li, Q., Xu, X.T., Cui, H., Pang, J.F., Wei, Z.B., Sun, Z.Q., Zhai, J.P., 2012. Comparison of two adsorbents for the removal of pentavalent arsenic from aqueous solutions. *J. Environ. Manag.* 98, 98–106.
- Li, S., Liu, W., Gu, S., Cheng, X., Xu, Z., Zhang, Q., 2009. Spatio-temporal dynamics of nutrients in the upper Han River basin, China. *J. Hazard. Mater.* 162, 1340–1346.
- Li, S., Xu, Z., Cheng, X., Zhang, Q., 2008. Dissolved trace elements and heavy metals in the Danjiangkou Reservoir, China. *Environ. Geol.* 55, 977–983.
- Maji, S.K., Pal, A., Pal, T., 2008. Arsenic removal from real-life groundwater by adsorption on laterite soil. *J. Hazard. Mater.* 151, 811–820.
- Makris, K.C., Harris, W.G., O'Connor, G.A., El-Shall, H., 2005. Long-term phosphorus effects on evolving physicochemical properties of iron and aluminum hydroxides. *J. Colloid. Interface Sci.* 287, 552–560.
- Ministry of Environmental Protection PR China, 2002. Environmental Quality Standards for Drinking Water (GB3838-2002) (in Chinese).
- Naoml, E.D., Patrick, L.B., 1991. Phosphorus sorption by sediments from a soft-water seepage lake. 2. Effects of pH and sediment composition. *Environ. Sci. Technol.* 25, 403–409.
- Peng, D., Liu, L., Hu, J.B., 2009. Vertical distribution and bio-availability sediments of Xuanwu Lake. *Water. Resour. Prot.* 25, 31–35 (in Chinese).
- Peng, J.F., Wang, B.Z., Song, Y.H., Yuan, P., Liu, Z.H., 2007. Adsorption and release of phosphorus in the surface sediment of a wastewater stabilization pond. *Ecol. Eng.* 31, 92–97.
- Penn, M.R., Auer, M.T., Van Orman, E.L., Korienek, J.J., 1995. Phosphorus diagenesis in lake sediments: investigation using fractionation techniques. *Mar. Freshw. Res.* 46, 89–99.
- Pu, X., Wu, Y., Zhang, Y., 2000. Nutrient limitation of phytoplankton in the Changjiang Estuary I Condition of nutrient limitation in Autumn. *Acta Oceanol. Sin.* 22, 60–66 (in Chinese).
- Ribeiro, D.C., Martins, G., Nogueira, R., Cruz, J.V., Brito, A.G., 2008. Phosphorus fractionation in volcanic lake sediments (Azores-Portugal). *Chemosphere* 70, 1256–1263.
- Ruban, V., López-Sánchez, J.F., Pardo, P., Rauret, G., Muntau, H., Quevauviller, P.H., 2001. Development of a harmonized phosphorus extraction procedure and certification of a sediment reference material. *J. Environ. Monitor.* 3, 121–125.
- Shao, Z.C., He, Q., Wang, W.J., 1998. Forms of aluminum in red soils. *Acta Pedol. Sin.* 35, 38–47 (in Chinese).
- Soon, Y.K., 1993. Fractionation of extractable aluminum in acid soils: a review and a proposed procedure. *Commun. Soil. Sci. Plant. Anal.* 24, 1683–1708.
- SPSS, 2003. Analytical Software. Statistical Package for the Social Sciences (SPSS). Headquarters 233 S. Wacker Drive, Chicago, IL.
- Tang, X.Q., Wu, M., Yang, W.J., Yin, W., Jin, F., Ye, M., Currie, N., Scholz, M., 2012. Ecological strategy for eutrophication control. *Water Air Soil Pollut.* 223, 723–737.
- Tian, J.R., Zhou, P.J., 2007. Phosphorus fractions of floodplain sediments and phosphorus exchange on the sediment-water interface in the lower reaches of the Han River in China. *Ecol. Eng.* 30, 264–270.
- Ulén, B., Snäll, S., 2007. Forms and retention of phosphorus in an illite-clay soil profile with a history of fertilisation with pig manure and mineral fertilizers. *Geoderma* 137, 455–465.
- Wang, L., Ma, C., 1999. A study on the environmental geology of the Middle Route Project of the South-north water transfer. *Eng. Geol.* 51, 153–165.
- Wang, S.R., Jin, X.C., Zhao, H.C., Zhou, X.N., Wu, F.C., 2007. Effect of organic matter on the sorption of dissolved organic and inorganic phosphorus in lake sediments. *Colloids. Surf. A* 297, 154–162.
- Wang, W., Hang, X.S., Zhang, Y.M., Yi, Y.L., 2011. Phosphorus adsorption of red clay and its mechanism. *J. Ecol. Rural Environ.* 27, 109–112 (in Chinese).
- Wang, W.J., 1995. Preliminary study on aluminum fractions in acid soil from Southern China. *Trop. Subtrop. Soil. Sci.* 4, 1–8 (in Chinese).
- Wang, Y., Shen, Z., Niu, J., Liu, R., 2009. Adsorption of phosphorus on sediments from the Three-Gorges Reservoir (China) and the relation with sediment compositions. *J. Hazard. Mater.* 162, 92–98.
- Wu, M., Huang, S.L., Wen, W., Sun, X.M., Tang, X.Q., Scholz, M., 2011. Nutrient distribution within and release from the contaminated sediment of Haihe River. *J. Environ. Sci.* 23, 1086–1094.
- Wu, M., Tang, X., Li, Q., Yang, W., Jin, F., Tang, M., Scholz, M., 2013. Review of ecological engineering solutions for rural non-point source water pollution control in Hubei Province, China. *Water Air Soil Pollut.* 224, 1561–1578.
- Xiong, W., Liao, Q., 2003. Influence of South to North Water Transfer Project's Middle Route on algae bloom in middle and lower reaches of Hangjiang River and countermeasures. *J. Yangtze. River. Sci. Res. Inst.* 20, 45–47 (in Chinese).
- Yamada, H., Mitsu, K., Kazuo, S., Hara, M., 1987. Suppression of phosphate liberation from sediment by using iron slag. *Water. Res.* 21, 325–333.
- Zak, D., Gelbrecht, J., 2002. Phosphorus retention at the redox interface of peatlands adjacent to surface waters. *Wasser. Boden.* 54, 71–76.
- Zhang, L., Wang, J.Q., Ma, Y.P., Chen, R., Ren, A.H., 2012. Phosphorus forms of different weathering degree rocks in Chaohu Lake area, China. *Environ. Sci.* 32, 1820–1825 (in Chinese).
- Zhou, A.M., Tang, H.X., Wang, S.W., 2005. Phosphorus adsorption on natural sediments: modeling and effects of pH and sediment composition. *Water. Res.* 39, 1245–1254.
- Zhou, Q., Gibson, C.E., Zhu, Y., 2001. Evaluation of phosphorus bioavailability in sediments of three contrasting lakes in China and the UK. *Chemosphere* 42, 221–225.